2018 Annual American Control Conference (ACC)
June 27–29, 2018. Wisconsin Center, Milwaukee, USA

Adaptive Attitude Control of a Dual-Rigid-Body Spacecraft with Unmodeled Nonminimum-Phase Dynamics

Zhanzhan Zhao[1], Gerardo Cruz[1], Taeyoung Lee[2], and Dennis S. Bernstein[1]

Abstract— **We consider control of a dual rigid-body spacecraft consisting of a bus and an appendage connected by a compliant joint. Thrust actuators are located on the spacecraft bus, and performance measurements are obtained from sensors on the appendage. This problem is challenging due to the flexibility of the joint and the noncolocation between the actuation and the performance variable. The goal is to motivate and investigate the challenges arising in control of nonminimum-phase (NMP) systems with rigid- and flexible-body dynamics. Exact equations of motion are derived for the spacecraft, and the invariant zeros of the linearized model are determined. This paper investigates the robustness of an adaptive control law to variations in the mass and inertia matrices of the bus and appendage as well as the geometry and joint stiffness. The adaptive controller uses no knowledge of the NMP dynamics.**

I. INTRODUCTION

Attitude control of flexible spacecraft is a long-studied problem that remains challenging due to uncertainty, nonlinearity, and dimensionality. Uncertainty arises due to imprecisely modeled dynamics; nonlinearity is due to large-angle and high-rate kinematics [1]; and high dimensionality reflects the continuum mechanics of flexible appendages and propellant slosh [2].

One of the difficulties of assessing the performance of control laws for these systems is the fact that models based on continuum mechanics depend on simplifying assumptions concerning properties of the material and the structure. In addition, the relevant partial differential equations are infinite dimensional, which ultimately requires approximation and truncation [3]. Since the model used for control design must depend on approximation and truncation, it is difficult to assess and compare the performance of attitude control laws. One way to overcome this difficulty is to derive a spacecraft model with discrete modes in place of continuum mechanics. A model of this type can be viewed as possessing idealized flexible modes that are exactly modeled.

The exact-modeling paradigm for investigating spacecraft attitude control laws was considered in [4] for a spacecraft consisting of a rigid bus with a discrete flexible mode assumed to be unmodeled. Retrospective cost adaptive control (RCAC) was applied. As shown in [5], RCAC uses limited modeling information: the leading sign of the numerator, the relative degree, and nonminimum-phase (NMP) zeros.

In the spirit of [4], the present paper considers a spacecraft consisting of two components, namely, a rigid bus and a rigid articulated appendage. These bodies are connected by a compliance that allows 3DOF relative rotation but no translation. The spacecraft sensors are assumed to be placed on the appendage, while thrusters apply torques to the spacecraft bus. The performance objective is thus to achieve attitude pointing of the appendage with actuation applied to the bus. This model may represent, for example, a telescope mounted on a spacecraft bus. As in the case of [4], this idealized flexible spacecraft amenable to exact modeling.

The challenging aspect of this spacecraft model is the fact that the actuation and performance variable are noncolocated. Because of noncolocation, control torques applied to the bus induce a rotation of the appendage relative to the bus that is initially in the opposite direction to the asymptotic angle. This undershoot phenomenon indicates NMP behavior, and linearization of the nonlinear equations of motion reveals the presence of NMP invariant zeros. The main goal of this paper is thus to investigate the performance of RCAC as applied to the dual-body spacecraft without using knowledge of the NMP dynamics as in [5].

II. DUAL RIGID-BODY SPACECRAFT MODEL

Consider a two-body spacecraft consisting of a rigid bus and a rigid appendage connected by a flexible joint as shown in Figure 1. The flexible joint allows longitudinal rotation of the appendage relative to the bus with torsional spring constant $\kappa_{\rm t}$ and lateral rotation of the appendage relative to the bus with bending spring constant $\kappa_{\rm b}$.

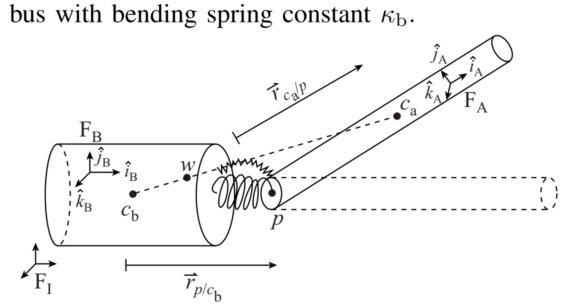

Fig. 1. Dual Rigid-Body Spacecraft. The bus and appendage are connected by a flexible joint that allows relative motion in torsion and bending.

The spacecraft is controlled by torque-generating actuators, such as thrusters, attached to the spacecraft bus. There is no onboard stored momentum. We define an inertial frame $\rm F_I$, a bus-fixed frame $\rm F_B$, and an appendage-fixed frame $\rm F_A$. Let $c_{\rm b}$ denote the center of mass of the bus, $c_{\rm a}$ denote the center of mass of the appendage, p denote the flexible joint connecting the bus and the appendage, and w denote the center of mass of the spacecraft. The location of the joint relative to the center of mass of the bus is denoted by $\overrightarrow{r}_{p/c_{\rm b}}$. Note that "$\overrightarrow{x}$" indicates a component-free physical vector.

[1]Department of Aerospace Engineering, University of Michigan, Ann Arbor, MI 48109
[2]Department of Mechanical and Aerospace Engineering, George Washington University, Washington DC 20052

It is assumed that, when the flexible joint is relaxed, the bus and appendage frames are aligned. In addition, as is shown in Figure 1, the bus and appendage frames are defined such that, when the flexible joint undergoes only torsion, then the appendage frame is related to the bus frame by a rotation around $\hat{\imath}_{\rm A}$. Likewise, when the flexible joint undergoes only bending, then the appendage frame is related to the bus frame by rotation around $\hat{\jmath}_{\rm A}$ and $\hat{k}_{\rm A}$.

The component-free tensor that rotates $\mathrm{F_I}$ to $\mathrm{F_B}$ is denoted by $\vec{R}_{\rm B/I}$. The angular velocity of the bus frame relative to the inertial frame is given by $\vec{\omega}_{\rm B/I}$, and the angular velocity of $\mathrm{F_A}$ relative to $\mathrm{F_I}$ is denoted by $\vec{\omega}_{\rm A/I}$. The rotation matrices, angular velocities, and position vectors are resolved in the bus and appendage frames as

$$R_{\rm b} \triangleq \vec{R}_{\rm B/I}\Big|_{\rm B}, \omega_{\rm b} \triangleq \vec{\omega}_{\rm B/I}\Big|_{\rm B}, \rho_{\rm b} \triangleq \vec{r}_{p/c_{\rm b}}\Big|_{\rm B}, \mu_{\rm b} \triangleq \hat{\jmath}_{\rm B}|_{\rm B}$$

$$R_{\rm a} \triangleq \vec{R}_{\rm A/I}\Big|_{\rm A}, \omega_{\rm a} \triangleq \vec{\omega}_{\rm A/I}\Big|_{\rm A}, \rho_{\rm a} \triangleq \vec{r}_{c_{\rm a}/p}\Big|_{\rm A}, \mu_{\rm a} \triangleq \hat{\jmath}_{\rm A}|_{\rm A}$$

For a vector $\vec{x}$, $\vec{x}\Big|_{\rm I} = R_{\rm b}\,\vec{x}\Big|_{\rm B}$, which shows that $R_{\rm b}$ transforms components of a vector resolved in $\mathrm{F_B}$ into the components resolved in $\mathrm{F_I}$.

The kinematic rotation equations are given by

$$\dot{R}_{\rm b} = R_{\rm b}\omega_{\rm b}^{\times}, \quad \dot{R}_{\rm a} = R_{\rm a}\omega_{\rm a}^{\times}, \tag{1}$$

where the superscript $\times$ indicates the skew-symmetric cross-product matrix operator. Since the bus is rigid, $\vec{r}_{p/c_{\rm b}}$ is fixed in $\mathrm{F_B}$. Similarly, $\vec{r}_{c_{\rm a}/p}$ is fixed in $\mathrm{F_A}$. Hence, $\dot{\rho}_{\rm b} = \dot{\rho}_{\rm a} = 0$. The configuration of the spacecraft is described by $R_{\rm b}$ and $R_{\rm a}$, and thus the configuration space is $\mathsf{SO}(3) \times \mathsf{SO}(3)$.

III. Lagrangian Mechanics on a Lie Group

The spacecraft may be subject to disturbance torques that vary along its orbit. However, we assume that the orbital and attitude dynamics are decoupled, and thus the center of mass w of the spacecraft can be viewed as an unforced particle, which provides a reference point for the rotational kinetic energy. In effect, the following analysis considers only the rotational kinetic energy of the spacecraft by ignoring the net force on the spacecraft and assuming that its translational kinetic energy is constant.

It follows from the definition of w that

$$\vec{r}_{c_{\rm b}/w}\Big|_{\rm I} = -\frac{m_{\rm a}}{m_{\rm a}+m_{\rm b}}(R_{\rm b}\rho_{\rm b} + R_{\rm a}\rho_{\rm a}), \tag{2}$$

where $m_{\rm a}$ is the mass of the appendage and $m_{\rm b}$ is the mass of the bus. It thus follows from (1)–(2) that

$$\overset{\rm I\bullet}{\vec{r}}_{c_{\rm b}/w}\Bigg|_{\rm I} = -\frac{m_{\rm a}}{m_{\rm a}+m_{\rm b}}(R_{\rm b}\omega_{\rm b}^{\times}\rho_{\rm b} + R_{\rm a}\omega_{\rm a}^{\times}\rho_{\rm a}). \tag{3}$$

Using (3), the kinetic energy of the bus $\mathcal{B}_{\rm b}$ relative to w with respect to $F_{\rm I}$ is given by

$$T_{\mathcal{B}_{\rm b}/w/{\rm I}} = \frac{1}{2}\omega_{\rm b}^{\rm T}J_{\rm b}\omega_{\rm b} + \alpha(R_{\rm b}\omega_{\rm b}^{\times}\rho_{\rm b} + R_{\rm a}\omega_{\rm a}^{\times}\rho_{\rm a})^2, \tag{4}$$

where $J_{\rm b} \in \mathbb{R}^{3\times 3}$ is the inertia matrix of the bus relative to its center of mass resolved in $\mathrm{F_B}$, and $\alpha \triangleq \frac{1}{2}m_{\rm b}(\frac{m_{\rm a}}{m_{\rm a}+m_{\rm b}})^2$.

Similarly, the appendage yields

$$\vec{r}_{c_{\rm a}/w}\Big|_{\rm I} = \frac{m_{\rm b}}{m_{\rm a}+m_{\rm b}}(R_{\rm b}\rho_{\rm b} + R_{\rm a}\rho_{\rm a}), \tag{5}$$

$$\overset{\rm I\bullet}{\vec{r}}_{c_{\rm a}/w}\Bigg|_{\rm I} = \frac{m_{\rm b}}{m_{\rm a}+m_{\rm b}}(R_{\rm b}\omega_{\rm b}^{\times}\rho_{\rm b} + R_{\rm a}\omega_{\rm a}^{\times}\rho_{\rm a}). \tag{6}$$

Using (6), the kinetic energy of the appendage is given by

$$T_{\mathcal{B}_{\rm a}/w/{\rm I}} = \frac{1}{2}\omega_{\rm a}^{\rm T}J_{\rm a}\omega_{\rm a} + \beta(R_{\rm b}\omega_{\rm b}^{\times}\rho_{\rm b} + R_{\rm a}\omega_{\rm a}^{\times}\rho_{\rm a})^2, \tag{7}$$

where $J_{\rm a} \in \mathbb{R}^{3\times 3}$ is the inertia matrix of the appendage relative to $c_{\rm a}$ resolved in $\mathrm{F_A}$, and $\beta \triangleq \frac{1}{2}m_{\rm a}(\frac{m_{\rm b}}{m_{\rm a}+m_{\rm b}})^2$.

Using (4) and (7), the kinetic energy of the spacecraft is

$$T_{\mathcal{B}_{\rm s}/w/{\rm I}} = \frac{1}{2}\omega_{\rm b}^{\rm T}J_{{\rm b}\gamma}\omega_{\rm b} + \frac{1}{2}\omega_{\rm a}^{\rm T}J_{{\rm a}\gamma}\omega_{\rm a} - \gamma\omega_{\rm b}^{T}\rho_{\rm b}^{\times}R_{\rm b}^{T}R_{\rm a}\rho_{\rm a}^{\times}\omega_{\rm a},$$

$$J_{{\rm b}\gamma} \triangleq J_{\rm b} - \gamma\rho_{\rm b}^{2\times}, \quad J_{{\rm a}\gamma} \triangleq J_{\rm a} - \gamma\rho_{\rm a}^{2\times}, \quad \gamma \triangleq \frac{m_{\rm a}m_{\rm b}}{m_{\rm a}+m_{\rm b}}.$$

The potential energy of the flexible joint is given by

$$U = \frac{\kappa_{\rm b}}{2}\theta_{\rm b}^2 + \frac{\kappa_{\rm t}}{2}\theta_{\rm t}^2, \tag{8}$$

where $\theta_{\rm b}$ is the angle between $\vec{r}_{p/c_{\rm b}}$ and $\vec{r}_{c_{\rm a}/p}$, $\kappa_{\rm b}$ is the bending spring stiffness, and $\theta_{\rm t}$ is the angle between $\hat{\jmath}_{\rm B}$ and $\hat{\jmath}_{\rm A}$, $\kappa_{\rm t}$ is the torsional spring stiffness. Hence,

$$U = \frac{\kappa_{\rm b}}{2}{\rm acos}^2\bar{\rho}_{\rm b}^{T}R_{\rm b}^{T}R_{\rm a}\bar{\rho}_{\rm a} + \frac{\kappa_{\rm t}}{2}{\rm acos}^2\bar{\mu}_{\rm b}^{T}R_{\rm b}^{T}R_{\rm a}\bar{\mu}_{\rm a}, \tag{9}$$

where $\bar{\rho}_{\rm b} \triangleq \frac{\rho_{\rm b}}{\|\rho_{\rm b}\|}$ and $\bar{\rho}_{\rm a} \triangleq \frac{\rho_{\rm a}}{\|\rho_{\rm a}\|}$ are the unit vectors along $\rho_{\rm b}$ and $\rho_{\rm a}$, respectively, and $\bar{\mu}_{\rm b} \triangleq \frac{\mu_{\rm b}}{\|\mu_{\rm b}\|}$ and $\bar{\mu}_{\rm a} \triangleq \frac{\mu_{\rm a}}{\|\mu_{\rm a}\|}$ are the unit vectors along $\mu_{\rm b}$ and $\mu_{\rm a}$, respectively.

It follows that the Lagrangian is

$$L = T_{\mathcal{B}_{\rm s}/w/{\rm I}} - U. \tag{10}$$

The derivatives of L with respect to $\omega_{\rm b}, \omega_{\rm a}, R_{\rm b}, R_{\rm a}$ are

$$\mathbf{D}_{\omega_{\rm b}}L = \frac{\partial L}{\partial \omega_{\rm b}} = J_{{\rm b}\gamma}\omega_{\rm b} - \gamma\rho_{\rm b}^{\times}R_{\rm b}^{T}R_{\rm a}\rho_{\rm a}^{\times}\omega_{\rm a}, \tag{11}$$

$$\mathbf{D}_{\omega_{\rm a}}L = \frac{\partial L}{\partial \omega_{\rm a}} = J_{{\rm a}\gamma}\omega_{\rm a} - \gamma\rho_{\rm a}^{\times}R_{\rm a}^{T}R_{\rm b}\rho_{\rm b}^{\times}\omega_{\rm b}, \tag{12}$$

$$\begin{aligned}\mathbf{D}_{R_{\rm b}}L = \frac{\partial L}{\partial R_{\rm b}} &= \kappa_{\rm b}\frac{\theta_{\rm b}}{\sin\theta_{\rm b}}R_{\rm a}\bar{\rho}_{\rm a}\bar{\rho}_{\rm b}^{T} + \kappa_{\rm t}\frac{\theta_{\rm t}}{\sin\theta_{\rm t}}R_{\rm a}\bar{\mu}_{\rm a}\bar{\mu}_{\rm b}^{T}\\ &\quad - \gamma R_{\rm a}\rho_{\rm a}^{\times}\omega_{\rm a}\omega_{\rm b}^{T}\rho_{\rm b}^{\times},\end{aligned} \tag{13}$$

$$\begin{aligned}\mathbf{D}_{R_{\rm a}}L = \frac{\partial L}{\partial R_{\rm a}} &= \kappa_{\rm b}\frac{\theta_{\rm b}}{\sin\theta_{\rm b}}R_{\rm b}\bar{\rho}_{\rm b}\bar{\rho}_{\rm a}^{T} + \kappa_{\rm t}\frac{\theta_{\rm t}}{\sin\theta_{\rm t}}R_{\rm b}\bar{\mu}_{\rm b}\bar{\mu}_{\rm a}^{T}\\ &\quad - \gamma R_{\rm b}\rho_{\rm b}^{\times}\omega_{\rm b}\omega_{\rm a}^{T}\rho_{\rm a}^{\times}.\end{aligned} \tag{14}$$

It follows from [6] that

$$(\mathsf{T}_e^*\mathsf{L}_{R_{\rm b}}\cdot\mathbf{D}_{R_{\rm b}}L)^{\rm T}\eta_0 = \langle\mathbf{D}_{R_{\rm b}}L, \delta R_{\rm b}\rangle = {\rm tr}\,(\mathbf{D}_{R_{\rm b}}L)^{\rm T}\delta R_{\rm b}, \tag{15}$$

where $\mathsf{T}_e^*\mathsf{L}_{R_{\rm b}}\cdot\mathbf{D}_{R_{\rm b}}L \in \mathbb{R}^3$ is the cotangent lift of the left translation [7], $\langle\mathbf{D}_{R_{\rm b}}L, \delta R_{\rm b}\rangle$ is the variation of the Lagrangian with respect to $R_{\rm b}$, and $\delta R_{\rm b}$ is the variation of

R_b. Furthermore, δR_b is given by

$$\delta R_\mathrm{b} = \frac{\mathrm{d}}{\mathrm{d}\varepsilon}\bigg|_{\varepsilon=0} R_\mathrm{b} e^{\varepsilon\eta_0} = R_\mathrm{b}\eta_0^\times, \tag{16}$$

where η_0 in (15) is the eigenaxis of δR_b. Using (13) and (16), it follows that

$$\begin{aligned}\langle \mathbf{D}_{R_\mathrm{b}} L, \delta R_\mathrm{b}\rangle &= \mathrm{tr}\,[(\mathbf{D}_{R_\mathrm{b}} L)^\mathrm{T} R_\mathrm{b}\eta_0^\times] \\ &= [\kappa_\mathrm{b}\frac{\theta_\mathrm{b}}{\sin\theta_\mathrm{b}}\bar\rho_\mathrm{b}^\times R_\mathrm{b}^T R_\mathrm{a}\bar\rho_\mathrm{a} + \kappa_\mathrm{t}\frac{\theta_\mathrm{t}}{\sin\theta_\mathrm{t}}\bar\mu_\mathrm{b}^\times R_\mathrm{b}^T R_\mathrm{a}\bar\mu_\mathrm{a} \\ &\quad + \gamma(\rho_\mathrm{b}^\times\omega_\mathrm{b})^\times R_\mathrm{b}^\mathrm{T} R_\mathrm{a}\rho_\mathrm{a}^\times\omega_\mathrm{a}]^\mathrm{T}\eta_0.\end{aligned} \tag{17}$$

Comparing (15) and (17) yields

$$\begin{aligned}\mathsf{T}_e^*\mathsf{L}_{R_\mathrm{b}}\cdot\mathbf{D}_{R_\mathrm{b}} L &= \frac{\kappa_\mathrm{b}\theta_\mathrm{b}}{\sin\theta_\mathrm{b}}\bar\rho_\mathrm{b}^\times R_\mathrm{b}^T R_\mathrm{a}\bar\rho_\mathrm{a} + \frac{\kappa_\mathrm{t}\theta_\mathrm{t}}{\sin\theta_\mathrm{t}}\bar\mu_\mathrm{b}^\times R_\mathrm{b}^T R_\mathrm{a}\bar\mu_\mathrm{a} \\ &\quad + \gamma(\rho_\mathrm{b}^\times\omega_\mathrm{b})^\times R_\mathrm{b}^\mathrm{T} R_\mathrm{a}\rho_\mathrm{a}^\times\omega_\mathrm{a}.\end{aligned} \tag{18}$$

Similarly,

$$\begin{aligned}\mathsf{T}_e^*\mathsf{L}_{R_\mathrm{a}}\cdot\mathbf{D}_{R_\mathrm{a}} L &= \frac{\kappa_\mathrm{b}\theta_\mathrm{b}}{\sin\theta_\mathrm{b}}\bar\rho_\mathrm{a}^\times R_\mathrm{a}^T R_\mathrm{b}\bar\rho_\mathrm{b} + \frac{\kappa_\mathrm{t}\theta_\mathrm{t}}{\sin\theta_\mathrm{t}}\bar\mu_\mathrm{a}^\times R_\mathrm{a}^T R_\mathrm{b}\bar\mu_\mathrm{b} \\ &\quad + \gamma(\rho_\mathrm{a}^\times\omega_\mathrm{a})^\times R_\mathrm{a}^\mathrm{T} R_\mathrm{b}\rho_\mathrm{b}^\times\omega_\mathrm{b}.\end{aligned} \tag{19}$$

The Euler-Lagrange equations on $\mathsf{SO}(3)\times\mathsf{SO}(3)$ [6] are given by

$$\frac{\mathrm{d}}{\mathrm{dt}}\mathbf{D}_{\omega_\mathrm{b}} L + \omega_\mathrm{b}^\times\mathbf{D}_{\omega_\mathrm{b}} L - \mathsf{T}_e^*\mathsf{L}_{R_\mathrm{b}}\cdot\mathbf{D}_{R_\mathrm{b}} L = M_\mathrm{b}, \tag{20}$$

$$\frac{\mathrm{d}}{\mathrm{dt}}\mathbf{D}_{\omega_\mathrm{a}} L + \omega_\mathrm{a}^\times\mathbf{D}_{\omega_\mathrm{a}} L - \mathsf{T}_e^*\mathsf{L}_{R_\mathrm{a}}\cdot\mathbf{D}_{R_\mathrm{a}} L = M_\mathrm{a}, \tag{21}$$

where M_b is the net torque on $\mathcal{B}_\mathrm{b}$ resolved in $\mathrm{F_B}$, and M_a is the net torque on $\mathcal{B}_\mathrm{a}$ resolved in $\mathrm{F_A}$. It follows that

$$M_\mathrm{b} = Bu + \tau_\mathrm{db}, \quad M_\mathrm{a} = \tau_\mathrm{da}, \tag{22}$$

where $u\in\mathbb{R}^3$ is the control torque vector resolved in $\mathrm{F_B}$, $B\in\mathbb{R}^{3\times3}$ determines the applied torque about each axis of $\mathrm{F_B}$ due to u, τ_db is disturbance torque on $\mathcal{B}_\mathrm{b}$ resolved in $\mathrm{F_B}$, and τ_da is disturbance torque on $\mathcal{B}_\mathrm{a}$ resolved in $\mathrm{F_A}$. It follows from (11), (12), (18), (19)-(22) that

$$\begin{aligned}J_{\mathrm{b}\gamma}\dot\omega_\mathrm{b} - \gamma\rho_\mathrm{b}^\times R_\mathrm{b}^T R_\mathrm{a}\rho_\mathrm{a}^\times\dot\omega_\mathrm{a} &= -\omega_\mathrm{b}^\times J_{\mathrm{b}\gamma}\omega_\mathrm{b} \\ &\quad + \gamma\rho_\mathrm{b}^\times R_\mathrm{b}^T R_\mathrm{a}\omega_\mathrm{a}^\times\rho_\mathrm{a}^\times\omega_\mathrm{a} + \kappa_\mathrm{b}\frac{\theta_\mathrm{b}}{\sin\theta_\mathrm{b}}\bar\rho_\mathrm{b}^\times R_\mathrm{b}^T R_\mathrm{a}\bar\rho_\mathrm{a} \\ &\quad + \kappa_\mathrm{t}\frac{\theta_\mathrm{t}}{\sin\theta_\mathrm{t}}\bar\mu_\mathrm{b}^\times R_\mathrm{b}^T R_\mathrm{a}\bar\mu_\mathrm{a} + Bu + \tau_\mathrm{db} \triangleq G_1,\end{aligned} \tag{23}$$

$$\begin{aligned}J_{\mathrm{a}\gamma}\dot\omega_\mathrm{a} - \gamma\rho_\mathrm{a}^\times R_\mathrm{a}^T R_\mathrm{b}\rho_\mathrm{b}^\times\dot\omega_\mathrm{b} &= -\omega_\mathrm{a}^\times J_{\mathrm{a}\gamma}\omega_\mathrm{a} \\ &\quad + \gamma\rho_\mathrm{a}^\times R_\mathrm{a}^T R_\mathrm{b}\omega_\mathrm{b}^\times\rho_\mathrm{b}^\times\omega_\mathrm{b} + \kappa_\mathrm{b}\frac{\theta_\mathrm{b}}{\sin\theta_\mathrm{b}}\bar\rho_\mathrm{a}^\times R_\mathrm{a}^T R_\mathrm{b}\bar\rho_\mathrm{b} \\ &\quad + \kappa_\mathrm{t}\frac{\theta_\mathrm{t}}{\sin\theta_\mathrm{t}}\bar\mu_\mathrm{a}^\times R_\mathrm{a}^T R_\mathrm{b}\bar\mu_\mathrm{b} + \tau_\mathrm{da} \triangleq G_2.\end{aligned} \tag{24}$$

We assume that the control thrusters are configured such that $B = I_3$.

Define $G = \begin{bmatrix} G_1^\mathrm{T} & G_2^\mathrm{T} & G_3^\mathrm{T} & G_4^\mathrm{T}\end{bmatrix}^\mathrm{T}\in\mathbb{R}^{3+3+9+9}$, where

$$G_3 \triangleq I_3\otimes(-\omega_\mathrm{b}^\times R_\mathrm{b}), \quad G_4 \triangleq I_3\otimes(-\omega_\mathrm{a}^\times R_\mathrm{a}). \tag{25}$$

The resulting equations of motion can be defined in terms of the state vector

$$x \triangleq \begin{bmatrix} \omega_\mathrm{b}^\mathrm{T} & \omega_\mathrm{a}^\mathrm{T} & \mathrm{vec}(R_\mathrm{b})^\mathrm{T} & \mathrm{vec}(R_\mathrm{a})^\mathrm{T}\end{bmatrix}^\mathrm{T}\in\mathbb{R}^{24}, \tag{26}$$

where "vec" is the column-stacking operator. Using (26) to rewrite (1), (23), and (24) yields

$$\dot x \triangleq F(x,u) \triangleq \begin{bmatrix} F_1^\mathrm{T} & F_2^\mathrm{T} & F_3^\mathrm{T} & F_4^\mathrm{T}\end{bmatrix}^\mathrm{T} = M(x)^{-1}G(x,u), \tag{27}$$

where $F_1, F_2\in\mathbb{R}^{3\times1}$, $F_3, F_4\in\mathbb{R}^{9\times1}$, and $M(x)\in\mathbb{R}^{24\times24}$ is defined by

$$M(x) \triangleq \begin{bmatrix}\hat M(x) & 0_{6\times18} \\ 0_{18\times6} & I_{18}\end{bmatrix}, \tag{28}$$

where the inertia matrix $\hat M\in\mathbb{R}^{6\times6}$ is defined by

$$\hat M(x) \triangleq \begin{bmatrix} J_{\mathrm{b}\gamma} & -\gamma\rho_\mathrm{b}^\times R_\mathrm{b}^T R_\mathrm{a}\rho_\mathrm{a}^\times \\ -\gamma\rho_\mathrm{a}^\times R_\mathrm{a}^T R_\mathrm{b}\rho_\mathrm{b}^\times & J_{\mathrm{a}\gamma}\end{bmatrix}. \tag{29}$$

The objective of this attitude control problem is to determine control inputs such that R_a follows commanded attitude trajectory given by rotation matrix R_d. The error between $R_\mathrm{a}(t)$ and $R_\mathrm{d}(t)$ is given in terms of the attitude-error rotation matrix

$$\tilde R \triangleq R_\mathrm{d}^\mathrm{T} R_\mathrm{a}, \quad \dot{\tilde R} = \tilde R\tilde\omega^\times, \tag{30}$$

where the angular velocity error $\tilde\omega$ is defined by

$$\tilde\omega \triangleq \omega_\mathrm{a} - \tilde R^\mathrm{T}\omega_\mathrm{d}, \tag{31}$$

where ω_d is the desired angular velocity of the appendage. For the output, which is the command-following error z, $\tilde R$ is represented by the vector S defined by

$$z \triangleq S(\tilde R) \triangleq \sum_{i=1}^3 a_i(\tilde R^\mathrm{T} e_i)\times e_i = \begin{bmatrix} a_3\tilde R_{32} - a_2\tilde R_{23} \\ a_1\tilde R_{13} - a_3\tilde R_{31} \\ a_2\tilde R_{21} - a_1\tilde R_{12}\end{bmatrix}\in\mathbb{R}^3, \tag{32}$$

where, for $i = 1,2,3$, $a_i\in\mathbb{R}$ are distinct and positive, and e_i is the ith column of I_3.

IV. Linearized Equations of Motion

We consider the equilibrium of (27) given by

$$(x_\mathrm{e}, u_\mathrm{e}) \triangleq \begin{bmatrix} 0_{1\times6} & e_1^\mathrm{T} & e_2^\mathrm{T} & e_3^\mathrm{T} & e_1^\mathrm{T} & e_2^\mathrm{T} & e_3^\mathrm{T} & 0_{1\times3}\end{bmatrix}^\mathrm{T}, \tag{33}$$

which represents the spacecraft at rest relative to $\mathrm{F_I}$ with body frames $\mathrm{F_B}$ and $\mathrm{F_A}$ aligned with $\mathrm{F_I}$ and zero control torque. Linearizing (27) at (33) yields

$$\delta\dot x = A_\mathrm{c}\delta x + B_\mathrm{c}\delta u, \tag{34}$$

$$A_\mathrm{c} \triangleq \frac{\partial F(x,u)}{\partial x}\bigg|_\mathrm{e} = \begin{bmatrix}\frac{\partial F_1}{\partial x}^\mathrm{T} & \frac{\partial F_2}{\partial x}^\mathrm{T} & \frac{\partial F_3}{\partial x}^\mathrm{T} & \frac{\partial F_4}{\partial x}^\mathrm{T}\end{bmatrix}^\mathrm{T}\bigg|_\mathrm{e}, \tag{35}$$

$$B_\mathrm{c} \triangleq \frac{\partial F(x,u)}{\partial u}\bigg|_\mathrm{e}. \tag{36}$$

Define $N \triangleq \rho_\mathrm{b}^\times\rho_\mathrm{a}^\times$, $Z \triangleq (J_{\mathrm{a}\gamma} - m_\mathrm{a}^2 N^\mathrm{T} J_{\mathrm{b}\gamma}^{-1} N)^{-1}$, $P \triangleq$

$ZN^{\mathrm{T}}J_{\mathrm{b}\gamma}^{-1}\bar{\rho}_{\mathrm{b}}^{\times}$, $R \triangleq ZN^{\mathrm{T}}J_{\mathrm{b}\gamma}^{-1}\bar{\mu}_{\mathrm{b}}^{\times}$, $Q \triangleq \gamma^2 N^{\mathrm{T}}J_{\mathrm{b}\gamma}^{-1}\rho_{\mathrm{b}}^{\times}E_{ji}\rho_{\mathrm{a}}^{\times}$, and $W \triangleq \rho_{\mathrm{a}}^{\times}E_{ij}\rho_{\mathrm{b}}^{\times}$, where $E_{ij} \triangleq e_i e_j^{\mathrm{T}}$. Assuming that the mass matrix $M(x)$ is positive definite, it follows that $\hat{M}(x)$ is also positive definite. In fact, Z is the $(2,2)$ block of $\hat{M}(x)^{-1}$, and thus Z is positive definite. Assuming $\frac{\theta_{\mathrm{b}}}{\sin\theta_{\mathrm{b}}} \approx 1$, $\frac{\theta_{\mathrm{t}}}{\sin\theta_{\mathrm{t}}} \approx 1$ and $\tau_{\mathrm{db}} = \tau_{\mathrm{da}} = 0_{3\times 1}$ yields

$$\left.\frac{\partial F_1(x,u)}{\partial x}\right|_{\mathrm{e}} = \left.\begin{bmatrix}\frac{\partial F_1}{\partial \omega_{\mathrm{b}}} & \frac{\partial F_1}{\partial \omega_{\mathrm{a}}} & \frac{\partial F_1}{\partial R_{\mathrm{b}_{ij}}} & \frac{\partial F_1}{\partial R_{\mathrm{a}_{ij}}}\end{bmatrix}\right|_{\mathrm{e}},$$

$$\begin{aligned}\left.\frac{\partial F_1}{\partial \omega_{\mathrm{b}}}\right|_{\mathrm{e}} &= \left.\frac{\partial F_1}{\partial \omega_{\mathrm{a}}}\right|_{\mathrm{e}} = 0_{3\times 3},\\ \left.\frac{\partial F_1}{\partial R_{\mathrm{b}_{ij}}}\right|_{\mathrm{e}} &= \gamma^2\kappa_{\mathrm{b}}J_{\mathrm{b}\gamma}^{-1}[NPE_{ji} + W^{\mathrm{T}}P\\ &\quad + NZ(WJ_{\mathrm{b}\gamma}^{-1}\bar{\rho}_{\mathrm{b}}^{\times} + QP + Q^{\mathrm{T}}P)]\bar{\rho}_{\mathrm{a}}\\ &\quad + \gamma\kappa_{\mathrm{b}}J_{\mathrm{b}\gamma}^{-1}[NZ\bar{\rho}_{\mathrm{a}}^{\times}E_{ij} + (NZQ + NZQ^{\mathrm{T}}\\ &\quad + W^{\mathrm{T}})Z\bar{\rho}_{\mathrm{a}}^{\times}]\bar{\rho}_{\mathrm{b}} + \kappa_{\mathrm{b}}J_{\mathrm{b}\gamma}^{-1}\bar{\rho}_{\mathrm{b}}^{\times}E_{ji}\bar{\rho}_{\mathrm{a}}\\ &\quad + \gamma^2\kappa_{\mathrm{t}}J_{\mathrm{b}\gamma}^{-1}[NRE_{ji} + W^{\mathrm{T}}R\\ &\quad + NZ(WJ_{\mathrm{b}\gamma}^{-1}\bar{\mu}_{\mathrm{b}}^{\times} + QR + Q^{\mathrm{T}}R)]\bar{\mu}_{\mathrm{a}}\\ &\quad + \gamma\kappa_{\mathrm{t}}J_{\mathrm{b}\gamma}^{-1}[NZ\bar{\mu}_{\mathrm{a}}^{\times}E_{ij} + (NZQ + NZQ^{\mathrm{T}}\\ &\quad + W^{\mathrm{T}})Z\bar{\mu}_{\mathrm{a}}^{\times}]\bar{\mu}_{\mathrm{b}} + \kappa_{\mathrm{t}}J_{\mathrm{b}\gamma}^{-1}\bar{\mu}_{\mathrm{b}}^{\times}E_{ji}\bar{\mu}_{\mathrm{a}}. \qquad (37)\end{aligned}$$

Replacing E_{ij} in (37) with E_{ji} yields $\left.\frac{\partial F_1}{\partial R_{\mathrm{a}_{ij}}}\right|_{\mathrm{e}}$. Also,

$$\begin{aligned}\left.\frac{\partial F_2}{\partial \omega_{\mathrm{b}}}\right|_{\mathrm{e}} &= \left.\frac{\partial F_2}{\partial \omega_{\mathrm{a}}}\right|_{\mathrm{e}} = 0_{3\times 3},\\ \left.\frac{\partial F_2}{\partial R_{\mathrm{b}_{ij}}}\right|_{\mathrm{e}} &= \gamma\kappa_{\mathrm{b}}[PE_{ji} + Z(WJ_{\mathrm{b}\gamma}^{-1}\bar{\rho}_{\mathrm{b}}^{\times} + QP\\ &\quad + Q^{\mathrm{T}}P)]\bar{\rho}_{\mathrm{a}}\\ &\quad + \kappa_{\mathrm{b}}Z[\bar{\rho}_{\mathrm{a}}^{\times}E_{ij} + (Q + Q^{\mathrm{T}})Z\bar{\rho}_{\mathrm{a}}^{\times}]\bar{\rho}_{\mathrm{b}}\\ &\quad + \gamma\kappa_{\mathrm{t}}[RE_{ji} + Z(WJ_{\mathrm{b}\gamma}^{-1}\bar{\mu}_{\mathrm{b}}^{\times} + QR\\ &\quad + Q^{\mathrm{T}}R)]\bar{\mu}_{\mathrm{a}}\\ &\quad + \kappa_{\mathrm{t}}Z[\bar{\mu}_{\mathrm{a}}^{\times}E_{ij} + (Q + Q^{\mathrm{T}})Z\bar{\mu}_{\mathrm{a}}^{\times}]\bar{\mu}_{\mathrm{b}}. \qquad (38)\end{aligned}$$

Replacing E_{ij} in (38) with E_{ji} yields $\left.\frac{\partial F_1}{\partial R_{\mathrm{a}_{ij}}}\right|_{\mathrm{e}}$. Also,

$$\begin{aligned}\left.\frac{\partial F_3(x,u)}{\partial x}\right|_{\mathrm{e}} &= \begin{bmatrix}-[e_1^{\times} & e_2^{\times} & e_3^{\times}]^{\mathrm{T}} & 0_{9\times 3} & 0_{9\times 18}\end{bmatrix},\\ \left.\frac{\partial F_4(x,u)}{\partial x}\right|_{\mathrm{e}} &= \begin{bmatrix}0_{9\times 3} & -[e_1^{\times} & e_2^{\times} & e_3^{\times}]^{\mathrm{T}} & 0_{9\times 18}\end{bmatrix},\\ \left.\frac{\partial F(x,u)}{\partial u}\right|_{\mathrm{e}} &= \begin{bmatrix}J_{\mathrm{b}\gamma}^{-1}B\\ \gamma ZN^{\mathrm{T}}J_{\mathrm{b}\gamma}^{-1}B\\ 0_{18\times 3}\end{bmatrix}. \qquad (39)\end{aligned}$$

The direction cosine matrix R_{a} can also be expressed in terms of 3-2-1 Euler angles ψ, θ, ϕ as

$$\begin{aligned}R_{\mathrm{a}} &= (\mathcal{O}_1(\phi)\mathcal{O}_2(\theta)\mathcal{O}_3(\psi))^{\mathrm{T}}\\ &= \begin{bmatrix}\mathrm{c}\theta\mathrm{c}\psi & \mathrm{s}\phi\mathrm{s}\theta\mathrm{c}\psi - \mathrm{c}\phi\mathrm{s}\psi & \mathrm{c}\phi\mathrm{s}\theta\mathrm{c}\psi + \mathrm{s}\phi\mathrm{s}\psi\\ \mathrm{c}\theta\mathrm{s}\psi & \mathrm{s}\phi\mathrm{s}\theta\mathrm{s}\psi + \mathrm{c}\phi\mathrm{c}\psi & \mathrm{c}\phi\mathrm{s}\theta\mathrm{s}\psi - \mathrm{s}\phi\mathrm{c}\psi\\ -\mathrm{s}\theta & \mathrm{s}\phi\mathrm{c}\theta & \mathrm{c}\phi\mathrm{c}\theta\end{bmatrix}, \qquad (40)\end{aligned}$$

$$\psi = \mathrm{atan}\frac{R_{\mathrm{a},21}}{R_{\mathrm{a},11}}, \quad \theta = \mathrm{asin}(-R_{\mathrm{a},31}), \quad \phi = \mathrm{atan}\frac{R_{\mathrm{a},32}}{R_{\mathrm{a},33}}.$$

Linearizing at $R_{\mathrm{a}} = I_3$ yields the local approximations

$$[\delta\phi \quad \delta\theta \quad \delta\psi]^{\mathrm{T}} \approx [\delta R_{\mathrm{a},32} \quad -\delta R_{\mathrm{a},31} \quad \delta R_{\mathrm{a},21}]^{\mathrm{T}}. \qquad (41)$$

V. Invariant Zeros of the Linearized System

Consider the inertia matrices

$$J_{\mathrm{b}} = \mathrm{diag}(100, 250/3, 50)\mathrm{kg\text{-}m}^2, J_{\mathrm{a}} = \mathrm{diag}(0.3, 1, 1)\mathrm{kg\text{-}m}^2.$$

$m_{\mathrm{a}} = 1$ kg, $m_{\mathrm{b}} = 100$ kg, $\kappa_{\mathrm{t}} = 10$ N/rad, $\kappa_{\mathrm{b}} = 100$ N/m, $\rho_{\mathrm{b}} = \rho_{\mathrm{a}} = [1\ 0\ 0]^{\mathrm{T}}$ m, and $\mu_{\mathrm{b}} = \mu_{\mathrm{a}} = [0\ 1\ 0]^{\mathrm{T}}$ m. Note that J_{b} and J_{a} are diagonal, which implies that $\mathrm{F_A}$ and $\mathrm{F_B}$ are principal axes of the bus and appendage, respectively. This assumption simplifies the subsequent analysis. Using $[\delta\phi \quad \delta\theta \quad \delta\psi]^{\mathrm{T}}$ in (41) as the output and constructing a minimal realization of the 3-input, 3-output linearized system (34), (41) of order 24 yields a 17th-order realization of the 3×3 transfer function

$$G_{\mathrm{tf}} = \begin{bmatrix}\frac{\widehat{\delta\phi}}{\hat{u}_1} & 0 & 0\\ 0 & \frac{\widehat{\delta\theta}}{\hat{u}_2} & 0\\ 0 & 0 & \frac{\widehat{\delta\psi}}{\hat{u}_3}\end{bmatrix}. \qquad (42)$$

The first row of G_{tf} accounts for the torsional motion of the appendage about its longitudinal axis. Note that, if $\kappa_{\mathrm{t}} = 0$, which models the case where the torsional spring is replaced by a frictionless bearing, then $\frac{\widehat{\delta\phi}}{\hat{u}_2} \equiv 0$. On the other hand, if $\kappa_{\mathrm{t}} >> 1$, which models the case where the appendage is connected rigidly to the bus in the longitudinal direction, then it can be shown numerically that $\frac{\widehat{\delta\phi}}{\hat{u}_2} \approx \frac{1}{(J_{\mathrm{a},22}+J_{\mathrm{b},22})s^2}$.

The $(2,2)$ entry of G_{tf}, which is the transfer function from u_2 to $\delta\theta$, has zeros ± 10.02, whereas, the $(3,3)$ entry of G_{tf}, which is the transfer function from u_3 to $\delta\psi$, has zeros ± 10.49. Consequently, G_{tf} has four invariant zeros, two of which are NMP.

Figure 2 shows how the NMP zeros of the $(2,2)$ and $(3,3)$ entries of G_{tf} depend on κ_{b}, κ_{t}, γ, $||\rho_{\mathrm{a}}||_2$, $||\rho_{\mathrm{b}}||_2$, $J_{\mathrm{a},11}$, $J_{\mathrm{a},22}$, $J_{\mathrm{a},33}$, $J_{\mathrm{b},11}$, $J_{\mathrm{b},22}$ and $J_{\mathrm{b},33}$ respectively.

To assess the accuracy of the linearized model, we compare the impulse response of the linearized system with the nonlinear system. The maximum deviation of the two systems after 250 steps is within 8%. The closeness of both systems show that the NMP behavior of the linearized system also gives rise in the nonlinear system.

VI. RCAC Algorithm [5]

RCAC uses a strictly proper input-output controller

$$u(k) \triangleq \sum_{i=1}^{n_{\mathrm{c}}} P_i(k)u(k-i) + \sum_{i=1}^{n_{\mathrm{c}}} Q_i(k)z(k-i) = \Phi(k)\theta(k),$$

where n_{c} is the controller order, $M_i(k) \in \mathbb{R}^{l_u\times l_u}$, $N_i(k) \in \mathbb{R}^{l_u\times l_y}$, Defining $l_\theta \triangleq l_u n_{\mathrm{c}}(l_u + l_y)$, then

$$\theta(k) \triangleq \mathrm{vec}\,[P_1(k)\cdots P_{n_{\mathrm{c}}}(k)\ Q_1(k)\cdots Q_{n_{\mathrm{c}}}(k)]^{\mathrm{T}} \in \mathbb{R}^{l_\theta},$$

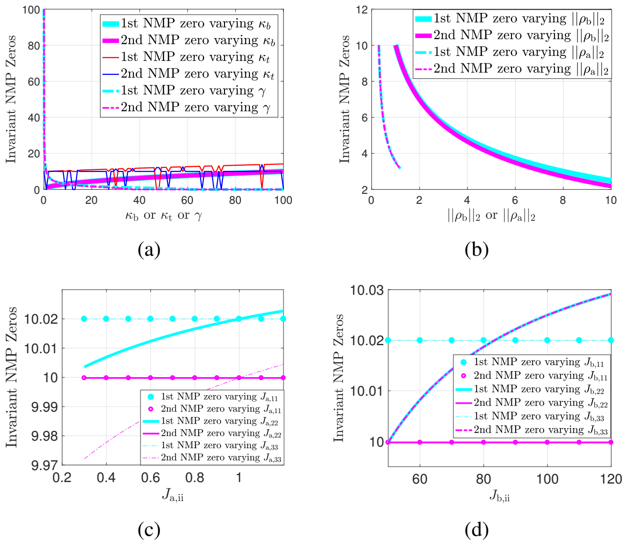

Fig. 2. NMP invariant zeros of the linearized system as a function of (a) κ_{b}, κ_{t}, and γ, (b) $||\rho_{\mathrm{a}}||_2$ and $||\rho_{\mathrm{b}}||_2$, (c) $J_{\mathrm{a},11}$, $J_{\mathrm{a},22}$, and $J_{\mathrm{a},33}$, (d) $J_{\mathrm{b},11}$, $J_{\mathrm{b},22}$, and $J_{\mathrm{b},33}$.

$$\Phi(k) \triangleq \begin{bmatrix} u(k-1) \\ \vdots \\ u(k-n_{\mathrm{c}}) \\ z(k-1) \\ \vdots \\ z(k-n_{\mathrm{c}}) \end{bmatrix}^{\mathrm{T}} \otimes I_{l_u} \in \mathbb{R}^{l_u \times l_\theta},$$

To update the controller coefficient vector $\theta(k)$, we define the retrospective performance

$$\hat{z}(k,\hat{\theta}) \triangleq z(k) + G_{\mathrm{f}}(\mathbf{q})[\Phi(k)\hat{\theta} - u(k)], \tag{43}$$

where $G_{\mathrm{f}} \in \mathbb{R}^{l_z \times l_u}$ is an FIR filter that captures the plant modeling information. The controller update $\theta(k+1) = \hat{\theta}$ is obtained by minimizing the retrospective cost function

$$J(k,\hat{\theta}) \triangleq \sum_{i=1}^{k} \eta_z \hat{z}(i,\hat{\theta})^{\mathrm{T}} \hat{z}(i,\hat{\theta}) + \sum_{i=1}^{k} \eta_u [\Phi(i)\hat{\theta}]^{\mathrm{T}} [\Phi(i)\hat{\theta}] + \eta_\theta [\hat{\theta} - \theta_0]^{\mathrm{T}} [\hat{\theta} - \theta_0], \tag{44}$$

where $\eta_z, \eta_u, \eta_\theta$ are positive scalars.

VII. Numerical Examples

In this paper, we set $G_{\mathrm{f}}(\mathbf{q}) = (1/\mathbf{q}) I_3$, where $\mathbf{q}$ is the forward shift operator. This choice means that RCAC uses no modeling information about the NMP zeros of the linearized plant. The identity matrix reflects the assumptions about the alignment of the actuators and sensors, but uses no knowledge of the dynamics of the spacecraft. The goal is to assess the closed-loop performance despite the absence of this modeling information. For all simulations, the plant is the exact nonlinear dynamics of the dual-rigid-body spacecraft given by (27) and (32).

To express the command-following error of the appendage attitude, $\tilde{R}$ in (30) is represented by the Rodrigues formula

$$\tilde{R}(\tilde{\theta},\xi) \triangleq (\cos\tilde{\theta}) I_3 + (1-\cos\tilde{\theta})\xi\xi^{\mathrm{T}} + (\sin\tilde{\theta})\xi^{\times}, \tag{45}$$

where $\xi \in \mathbb{R}^3$ is the eigenaxis resolved in $\mathrm{F_A}$ and $\tilde{\theta} \in (-\pi,\pi]$ is the eigenangle. In terms of the appendage attitude $R_{\mathrm{a}}(t)$ and the desired attitude $R_{\mathrm{d}}(t)$, attitude-error metric is given by the eigenangle of $\tilde{R}$

$$\tilde{\theta}(t) = \cos^{-1}(\tfrac{1}{2}[\mathrm{tr}\,\tilde{R}(t) - 1]). \tag{46}$$

Using the Rodrigues formula, R_{d} can be represented by eigenangle θ_{d} and eigenaxis ξ_{d} resolved in $\mathrm{F_A}$.

As in [4], the settling-time metric is defined as

$$T_{\mathrm{s}} = \min\{t > ih : \text{for all}\, i \in 1,\ldots,400, \tilde{\theta}(t-ih) < 3\,\mathrm{deg}\},$$

where $h = 0.1$ s is the integration step length. The final error metric is the average of $\tilde{\theta}(t)$ over the last 1 s of simulation.

We consider R2R maneuvers for command following with disturbance rejection, where the desired attitude of the appendage is a fixed attitude in the inertial frame. The spacecraft is initially at rest. The numerical values in Section V are used in this section.

A. R2R Maneuvers with Disturbances

1) Command Following: In Figure 3, the disturbance is set to $\tau_{\mathrm{db}} = \tau_{\mathrm{da}} = [0\ 0.4\sin(100t)\ 0]^{\mathrm{T}}$. Various commanded motions of the appendage, with desired eigenangle θ_{d} varying from $-180°$ to $180°$ around the desired eigenaxes ξ_{d} $[1\ 1\ 1]^{\mathrm{T}}, [1\ 0\ 0]^{\mathrm{T}}, [0\ 1\ 0]^{\mathrm{T}}, [0\ 0\ 1]^{\mathrm{T}}$ are tested.

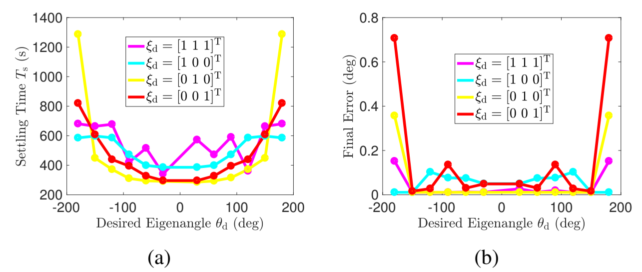

Fig. 3. For the performance weights $\eta_z = 1$, $\eta_u = 0.2$, and $\eta_\theta = 0.01$, $n_{\mathrm{c}} = 2$, $\tau_{\mathrm{db}} = \tau_{\mathrm{da}} = [0\ 0.4\sin(100t)\ 0]^{\mathrm{T}}$, (a) shows the settling time T_{s} as a function of the desired eigenangle θ_{d} and eigenaxis ξ_{d}, and (b) shows the corresponding final error.

2) Stochastic Disturbance: The components of the external torque disturbances τ_{db} and τ_{da} are both Gaussian white noise with covariance matrix $0.001 I_3$ and mean $[0.1\ 0.1\ 0.1]^{\mathrm{T}}$. The command for the appendage is a 150-deg rotation about $\xi_{\mathrm{d}} = [1\ 1\ 1]^{\mathrm{T}}$. Figure 4 shows that RCAC achieves the desired appendage attitude.

B. Robustness Test

1) Robustness to Off-Diagonal Inertia Matrix: As is shown in Figure 5, to account for the case when $\mathrm{F_B}$ is not the principal-axis frame of the bus relative to c_{b}, we rotate the bus inertia matrix by eigenangle θ about body-fixed eigenaxis

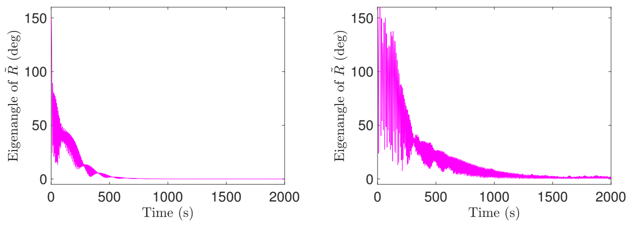

Fig. 4. For the performance weights $\eta_z = 1$, $\eta_u = 0.2$, and $\eta_\theta = 0.01$, $n_\mathrm{c} = 2$, (a) shows $\tilde{\theta}$ as a function of time without stochastic disturbance. The settling time is 506 s, and the final error is 1.5×10^{-5} deg. The maximum control input is 20.6 N-m. (b) shows $\tilde{\theta}$ as a function of time with stochastic disturbance. The settling time is 1506 s, and the asymptotic error is 1.72 deg. The maximum control input is 23.3 N-m.

$n = [1\ 1\ 1]^\mathrm{T}$. The rotated inertia matrix J_R is defined as

$$J_\mathrm{R} \stackrel{\triangle}{=} R(\theta, n)^\mathrm{T} J_\mathrm{b} R(\theta, n), \tag{47}$$

where $R(\theta, n)$ is obtained using Rodrigues formula.

2) Robustness to Diagonal Inertia Matrix Variations: Now, we assume that $\mathrm{F_B}$ is the principal-axis frame of the bus, and that $\mathrm{F_A}$ is the principal-axis frame of the appendage. We define the nominal inertia cases as $\bar{J}_1 = \mathrm{diag}(100, 100, 100)$, $\bar{J}_2 = \mathrm{diag}(100, 100, 50)$, $\bar{J}_3 = \mathrm{diag}(100, 250/3, 50)$, where, according to [4], $\bar{J}_1$, $\bar{J}_2$, and $\bar{J}_3$ correspond to the inertia matrix of a sphere, cylinder, and cuboid, respectively. The varied inertia matrix is

$$J_{ij}(\alpha) = \beta[(1 - \alpha)\bar{J}_i + \alpha\bar{J}_j], \tag{48}$$

where $i, j \in \{(3, 1), (3, 2), (1, 3)\}$ for $\alpha \in [0, 1]$, and $\beta > 0$. $J_{31}(\alpha)$ indicates the varying of inertia from the cuboid to sphere. $J_{32}(\alpha)$ is the inertia varying from the cuboid to cylinder. $J_{13}(\alpha)$ is varied from the sphere to cuboid.

In Figure 6 (a)-(b), we vary the bus inertia, that is $J_\mathrm{b} = J_{ij}(\alpha)$, with $\beta = 1$. Similarly, in Figure 6 (c)-(d), we vary the appendage's inertia, that is $J_\mathrm{a} = J_{ij}(\alpha)$, with $\beta = 0.01$.

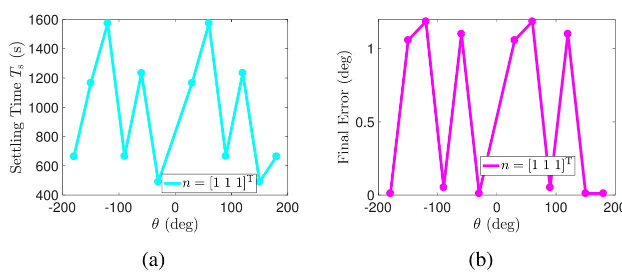

Fig. 5. For the performance weights $\eta_z = 1$, $\eta_u = 0.2$, $\eta_\theta = 0.01$, $n_\mathrm{c} = 2$, $\xi_\mathrm{d} = [1\ 1\ 1]^\mathrm{T}, \theta_\mathrm{d} = 150\,\mathrm{deg}$, and $\tau_\mathrm{db} = \tau_\mathrm{da} = [0\ 0.4\sin(100t)\ 0]^\mathrm{T}$, (a) shows the settling time T_s as a function of θ, and (b) shows the corresponding final error.

3) Robustness to Variations of Other Configuration Parameters of the Spacecraft: In Figure 7, we vary the spring stiffness κ_b and κ_t.

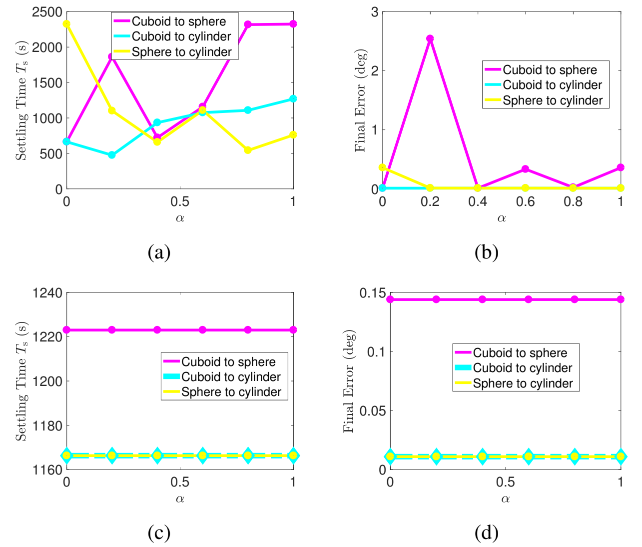

Fig. 6. For the performance weights $\eta_z = 1$, $\eta_u = 0.2$, $\eta_\theta = 0.01$, $n_\mathrm{c} = 2$, $\xi_\mathrm{d} = [1\ 1\ 1]^\mathrm{T}, \theta_\mathrm{d} = 150\,\mathrm{deg}$, and $\tau_\mathrm{db} = \tau_\mathrm{da} = [0\ 0.4\sin(100t)\ 0]^\mathrm{T}$, (a) shows the settling time T_s as a function of α with the bus inertia varied in 3 ways, and (b) shows the corresponding final error. (c) shows the settling time T_s as a function of α with the appendage inertia varied in 3 ways, and (d) shows the corresponding final error.

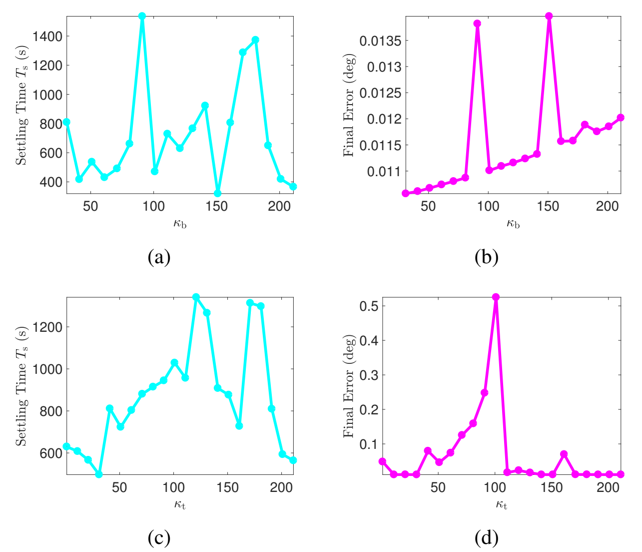

Fig. 7. For the performance weights $\eta_z = 1$, $\eta_u = 0.2$, $\eta_\theta = 0.01$, $n_\mathrm{c} = 2$, $\xi_\mathrm{d} = [1\ 1\ 1]^\mathrm{T}, \theta_\mathrm{d} = 150\,\mathrm{deg}$, and $\tau_\mathrm{db} = \tau_\mathrm{da} = [0\ 0.4\sin(100t)\ 0]^\mathrm{T}$, (a) shows the settling time T_s as a function of κ_b, and (b) shows the corresponding final error. (c) shows the settling time T_s as a function of κ_t, and (d) shows the corresponding final error.

References

[1] Hughes, P. C., *Spacecraft Attitude Dynamics*, John Wiley, 1986.

[2] Bryson, A. E., *Control of Spacecraft and Aircraft*, Princeton University Press, 1994.

[3] Du, H. and Li, S., "Attitude synchronization control for a group of flexible spacecraft," *Automatica*, Vol. 50, No. 2, 2014, pp. 646–651.

[4] Camblor, M., Xie, A., Cruz, G., Esteban, S., Lee, T., and Bernstein, D. S., "A Numerical Comparison of Inertia-Free Attitude Control Laws for a Spacecraft with a Discrete Flexible Mode," *Proc. AIAA Guid. Nav. Contr. Conf.*, Boston, MA, August 2013, AIAA-2013-4562.

[5] Rahman, Y., Xie, A., and Bernstein, D. S., "Retrospective Cost Adaptive Control: Pole Placement, Frequency Response, and Connections with LQG Control," *IEEE Contr. Sys. Mag.*, October 2017, pp. 28–69.

[6] Lee, T., Leok, M., and McClamroch, N. H., *Global Formulations of Lagrangian and Hamiltonian Dynamics on Manifolds*, Springer, 2018.

[7] Marsden, J. E. and Ratiu, T. S., *Introduction to Mechanics and Symmetry: A Basic Exposition of Classical Mechanical Systems*, Springer, 1999.